Supporting information

SPIONs nano-devices based on Fe_3O_4 coated by megluminic ligands for the adsorption of metal anions from water

Stefano Scurti[1], Sandro Dattilo[2*], David Gintsburg[1], Luigi Vigliotti[3], Aldo Winkler [4], Sabrina Carola Carroccio[2], Daniele Caretti[1]

[1] Dipartimento di Chimica Industriale "Toso Montanari", University of Bologna, Viale Risorgimento 4, 40136 Bologna, Italy
[2] Istituto per i Polimeri, Compositi e Biomateriali, CNR-IPCB, Via Paolo Gaifami 18, 95126 Catania, Italy
[3] Istituto di Scienze Marine, ISMAR-CNR, Via P. Gobetti 101, 40129 Bologna, Italy
[4] Istituto Nazionale di Geofisica e Vulcanologia, Via di Vigna Murata, 605, 00143 Rome, Italy

4-vinyl-benzyl-meglumine (VbMEG) characterization

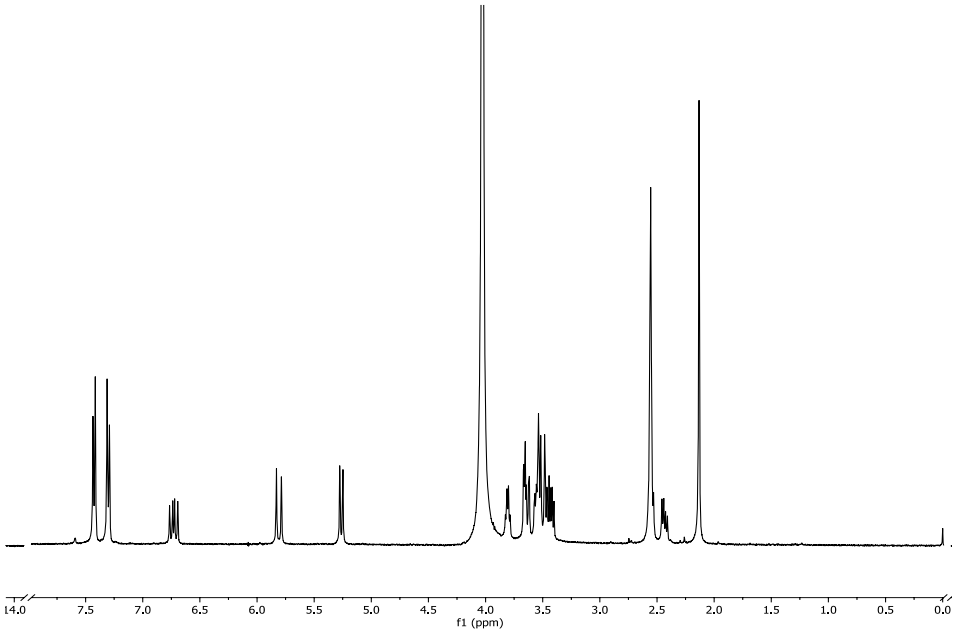

Figure S1: [1]H-NMR e spectra of (4-vinylbenzyl)-meglumine (VbMEG) in d_6-DMSO-D_2O

The purified VbMEG monomer was characterized by [1]H-NMR and FT-IR spectroscopy as reported in Figure S1 and Figure S2, respectively. By NMR spectrum, the presence of the para-disubstituted aromatic ring linked to the meglumine moiety was observed at 7.5 ppm. Additionally, typical segnals distribution related to C=C bond and the overlapped aliphatic hydrogen signals deraived from meglumic group were observed in the region ranging from 5.0 to 7.0 ppm and from 2.5 to 3.8 ppm, respectively. Moreover, the absence of the signals realted to the starting reagents confirmed that efficient purification had taken place.

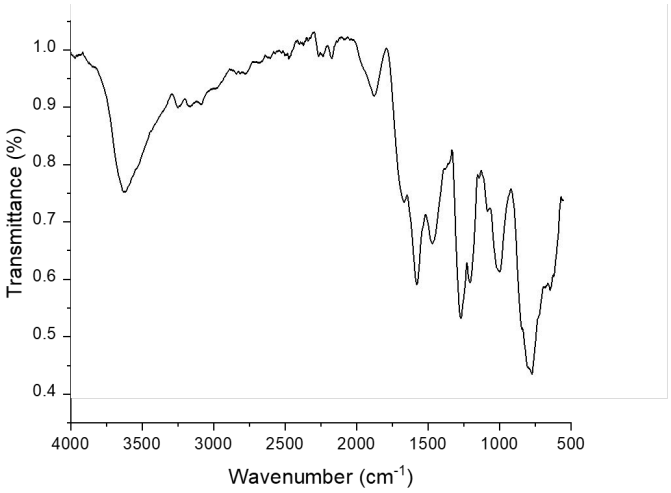

Figure S2: Infrared spectra of (4-vinylbenzyl)-meglumine (VbMEG)

By FT-IR spectra of MEG monomer diagnostic bands at 3400−3100, 3000−2780, and 1100 cm^{-1} related to the stretching vibrations of O−H, C−H, and C−O groups, respectively were observed. Moreover, the characteristic peaks at 1630 and 1390 cm^{-1} indicate the presence of the C=C aromatic stretching and the tertiary C−N stretching modes.

Poly-(4-vinyl-benzyl)-meglumine (p-VbMEG) characterization

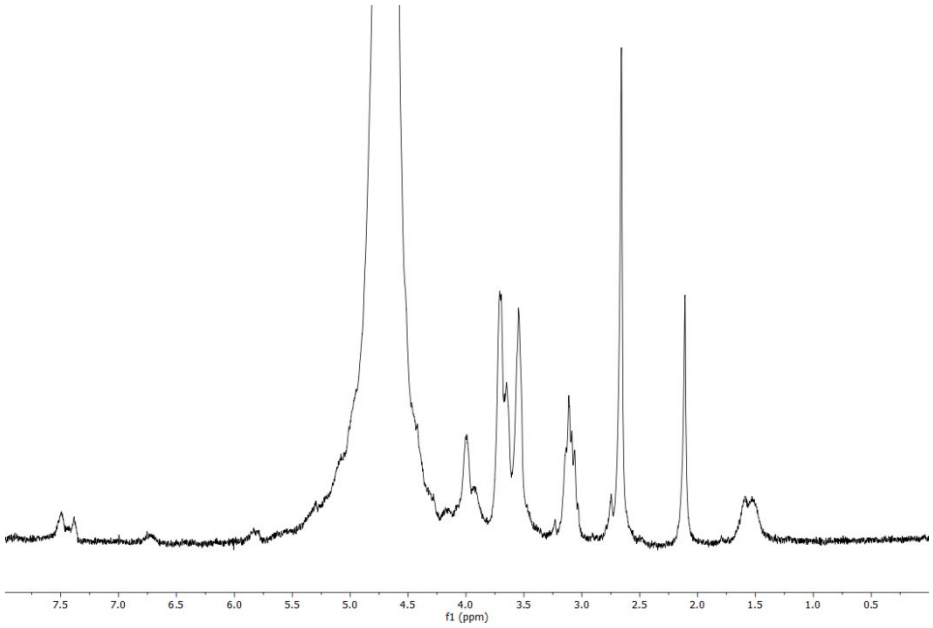

Figure S3: ^{1}H-NMR spectra of poly-(4-vinylbenzyl)-meglumine (pVbMEG) in D_2O

Poly-(4-vinylbenzyl)-meglumine synthesized was characterized by NMR and FT-IR spectroscopy as reported in Figure S3 and S4, respectively. Although, by ^{1}H-NMR spectra a little amount of starting monomer not reacted can be observed, the presence of wide signals confirmed the polymerization reaction. Moreover, the distribution related to the presence of meglumine groups was observed in the range from 4-2 ppm.

In Figure S4 FT-IR spectrum of pVbMEG was reported to confirm the polymerization reaction. The spectrum presents characteristic diagnostic bands at 3400−3100, 3000−2780, 1650, and 1100 cm^{-1} related to the stretching vibrations of O−H, C−H, C=O, and C−O group, respectively. In addition, the characteristic peaks in the regions 1600-1475 cm^{-1} and 1450-1390 cm^{-1} evidenced the typical C=C aromatic stretching and the tertiary and secondary C−N stretching modes.

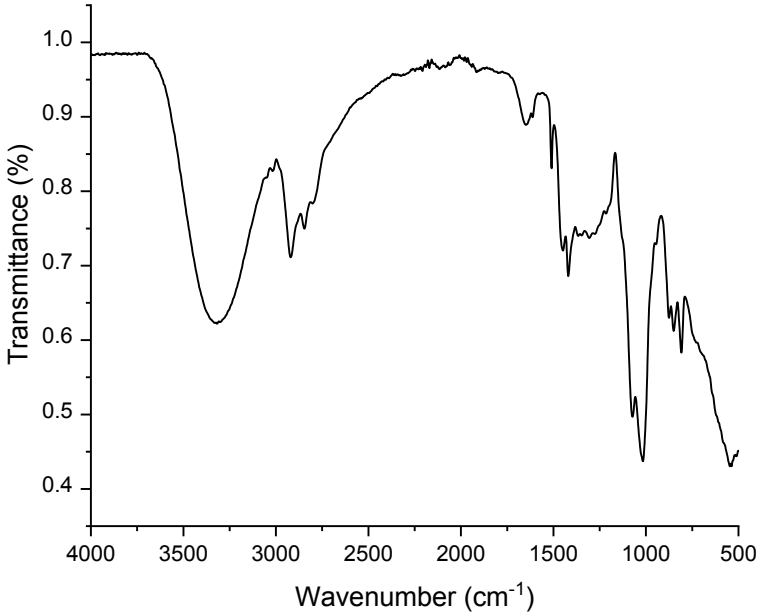

Figure S4: Infrared spectra of poly-(4-vinylbenzyl)-MEG (pVbMEG)

Figure S5 shows the termogram of pVbMEG. In agreement with the previous data [1], the sample exhibits two dinstinct thermal degradation steps. The first around to 310 °C can derive from the decomposition of meglumine moieties. Instead, at higher temperatures, the thermal degradation of the polymeric chains took place in the range of 412–435 °C.

The presence of aromatic rings bring to the formation of char, the value of the residue is nearly 20 %.

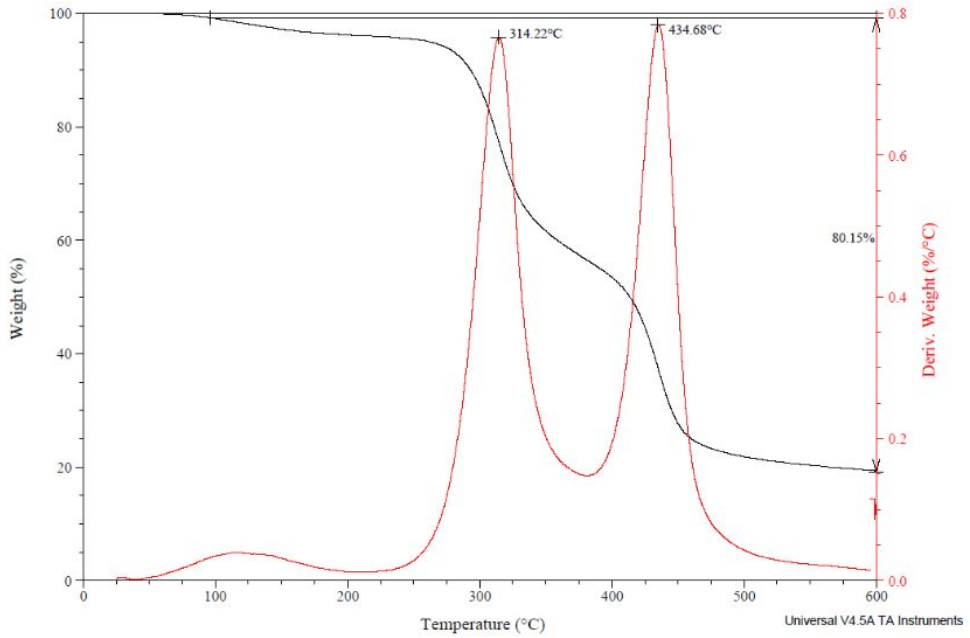

Figure S5:TGA and dTGA profiles of poly-(4-vinyl-benzyl)-meglumine (p-VbMEG)

Fe_3O_4 nanostructured materials characterization

The TGA analysis were widely discussed in 3.2.3 paragraph in the main text. Despite, the complexity of nanostructured materials is possible observed the degradation steps related to the inorganic phase like the degradation temperatures of the organic coatings, in this way it's can be possible to confirmed the correct functionalization of SPIONs nanoparticles. Moreover, by TGA carried out in oxidative atmosphere the amount of organic coating has been observed and calculated.

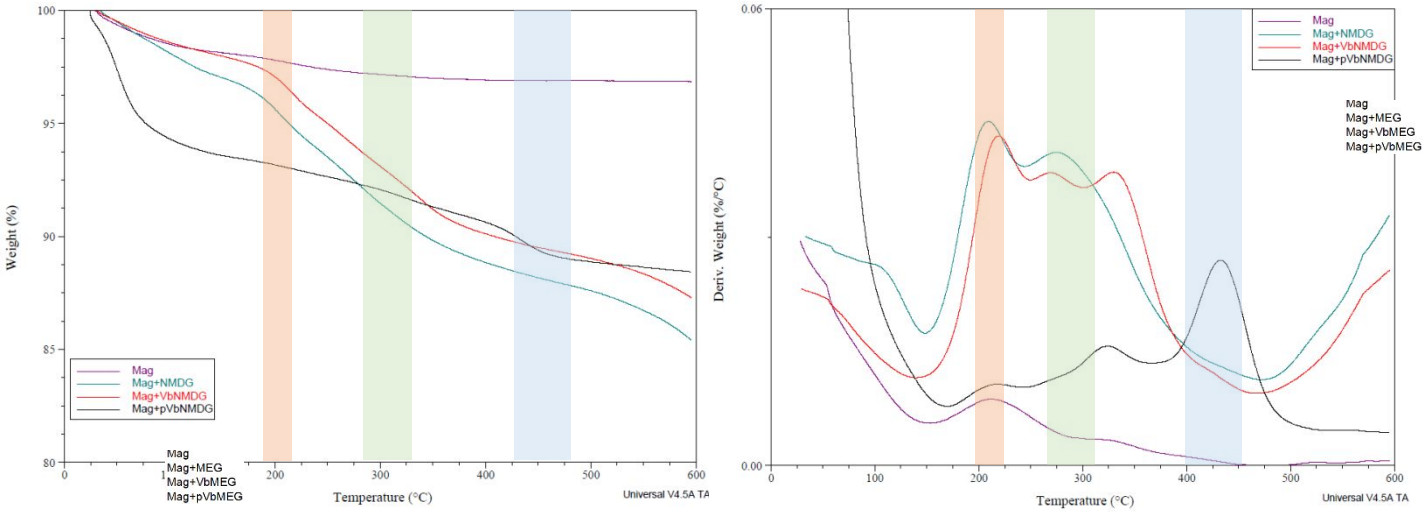

Figure S6: TGA and dTGA profiles in N_2 atmosphere for MEG loaded on Fe3O4; VbMEG loaded on Fe3O4 and poly-VbMEG loaded on Fe3O4

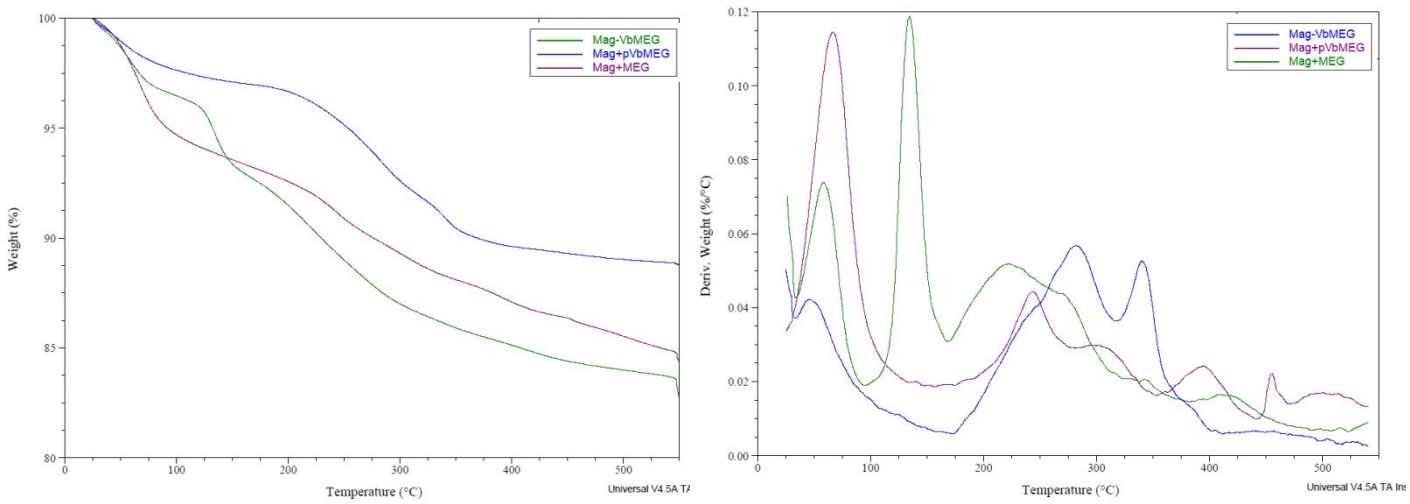

Figure S7 : TGA and dTGA profiles in oxidative atmosphere for the bare magnetite nanoparticles; MEG loaded on Fe3O4; VbMEG loaded on Fe3O4 and poly-VbMEG loaded on Fe3O4

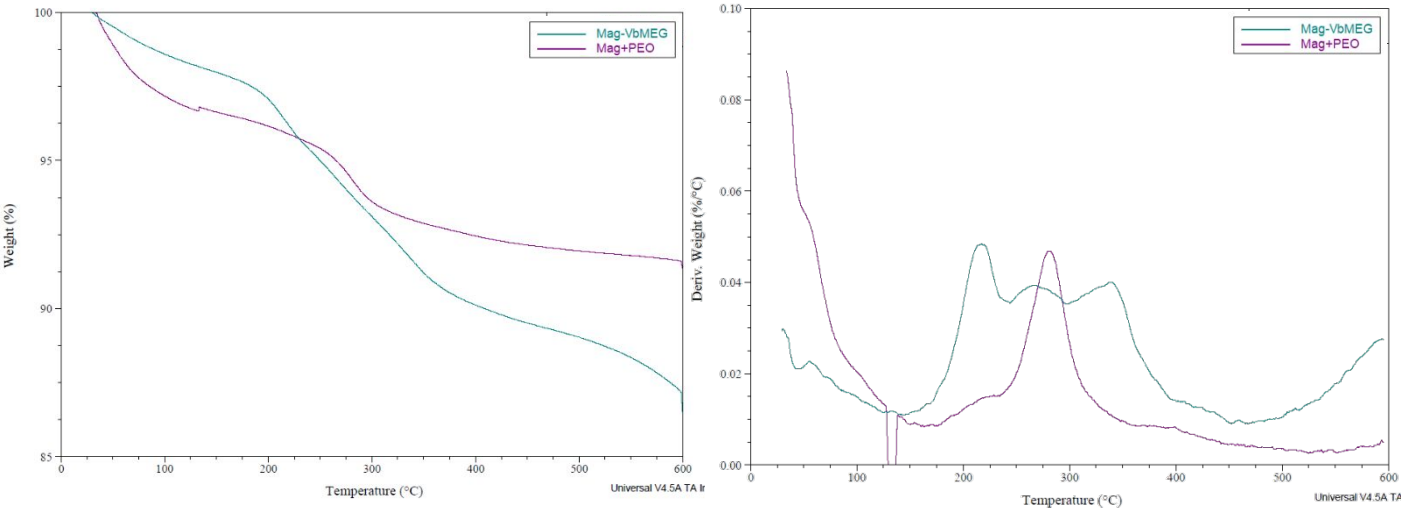

Figure S8: TGA and dTGA profiles in N_2 atmosphere for the PEO and VbMEG loaded on Fe3O4

Thermogravimetric analysis (TGA) in nitrogen atmosphere was carried out to evaluate the ligands exchange reaction in PEO-Fe_3O_4 nanostructured materials. For the PEO functionalized material typical degradation step at 290 °C related to poly-ethylene oxide decomposition was observed accordingly with the temperature reported in literature.[2] After the exchange with the MEG monomer, different degradative steps were observed in the range from 250-350 °C due to the thermal decomposition of meglumine moiety.

Scanning Electron Microscopy (SEM)

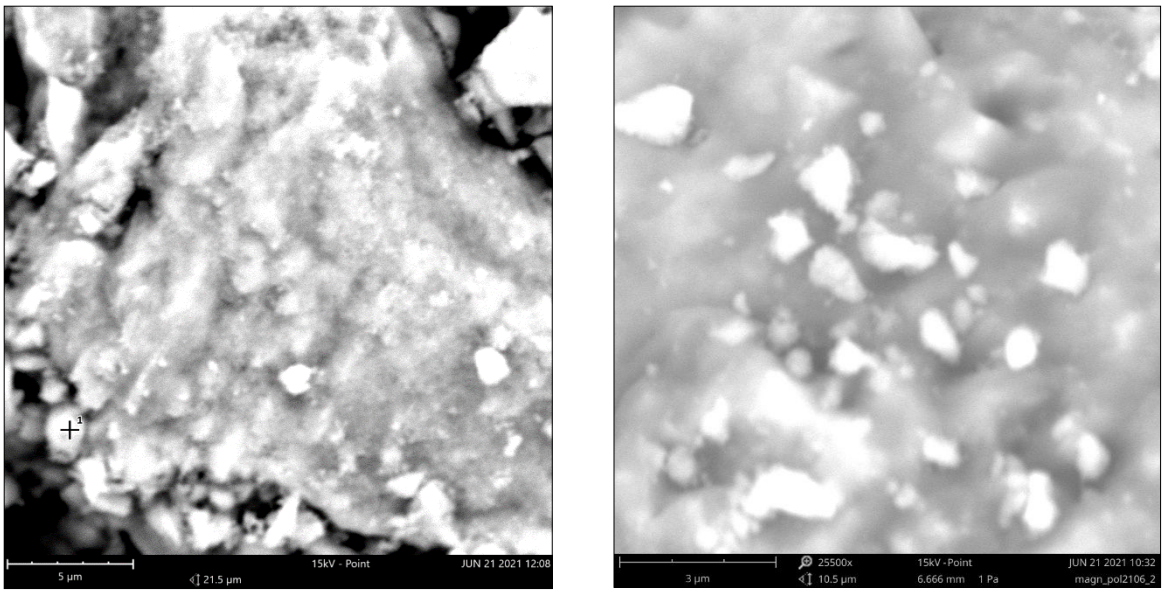

Figure S9: SEM images related to bare Fe3O4 (left) and pVbMEG loaded on Fe3O4 (right)

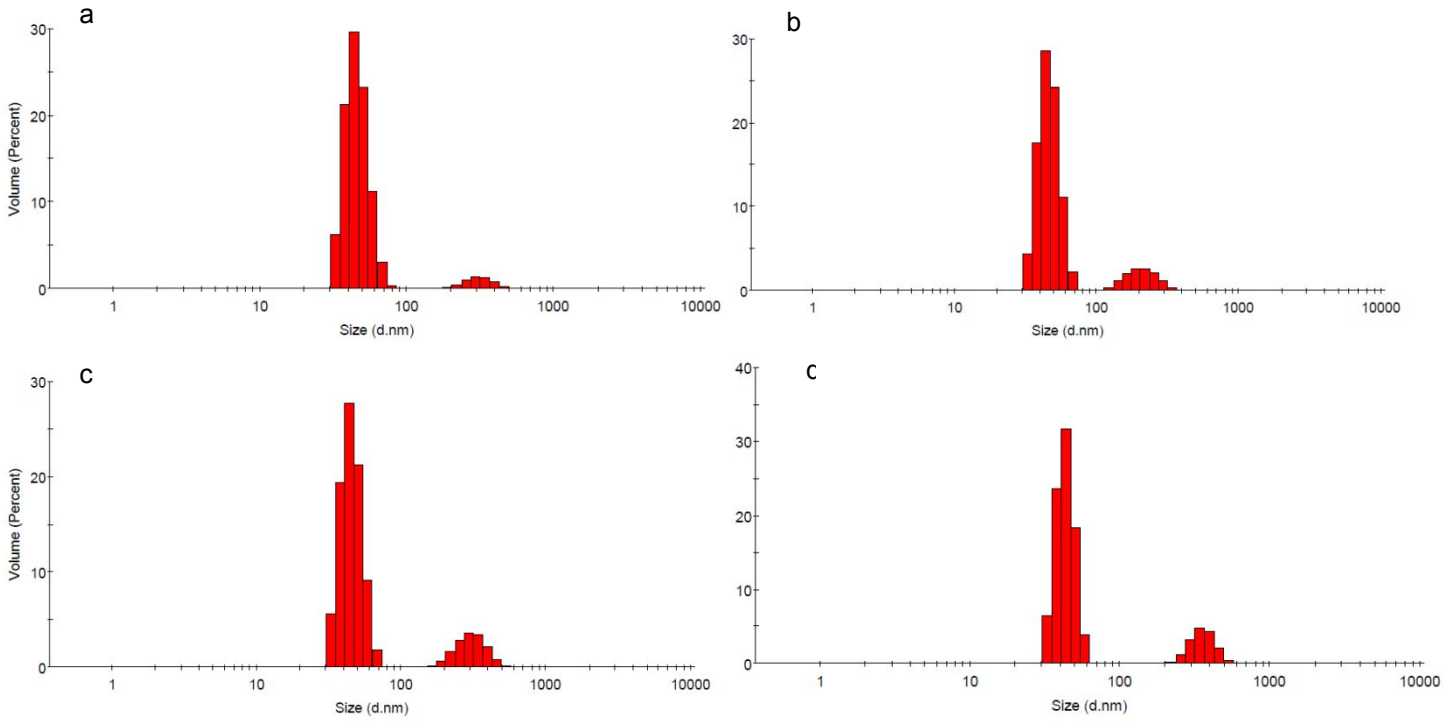

Figure S10: DLS diameter (nm) distributions related to bare Fe3O4 (a); MEG loaded on Fe3O4 (b); VbMEG loaded on Fe3O4 (c) and pVbMEG loaded on Fe3O4 (d)

Adsorption test

Different kinetic models were applied to investigate the adsorption process of the synthesized nanostructured materials. In particular pseudo-first order, pseudo-second order and intraparticle diffusion models have been used.[3–5] Firstly, the adsorption equilibrium capacity (Q_e) was calculated by the following equation:

$$Q_e = \frac{(C_o - C_e) \cdot V}{W} \qquad (1)$$

where C_0 (mg/L) is the metal initial concentration, C_e (mg/L) is its concentration at the equilibrium, V (L) is the volume of water used and W (g) is the weight of adsorbent nanomaterials used during the experiments. The pseudo-first order model for heterogeneous solid–liquid systems is formulated as follows:

$$\ln(Q_e - Q_t) = lnQ_e - k_1 t \qquad (2)$$

where Q_e and Q_t (mg/g) are the amounts of metal ions adsorbed at equilibrium and time t (min) respectively, by using as initial conditions $Q_{t=0}$ at t=0. The constant rate k_1 (min^{-1}) is obtained by plotting $\ln(Q_e-Q_t)$ versus time (min).

In addition, the pseudo-second order kinetic model is used to investigate the kinetic behaviour by the following equation:

$$\frac{t}{Q_t} = \frac{1}{k_2 Q_e^2} + \frac{t}{Q_e} \qquad (3)$$

By plotting the experimental data t/Q_t versus time, Q_e and k_2 were assessed from both the slope and intercept, respectively.

The last model used to evaluate the adsorption process is the intraparticle diffusion one described with the following equation:

$$Q_t = k_i\sqrt{t} + C \qquad (4)$$

where k_i is the intraparticle diffusion rate constant (mg $g^{-1}h^{-0.5}$). By plotting the amount of metal ions adsorbed against the square root of the contact time, it can be possible to evaluate the influence of the interparticle diffusion into the rate limiting-step.[5]

Moreover, adsorption models were used to rationalize the equilibrium adsorption by the isotherms and therefore investigate the adsorption information, such as the adsorption mechanisms, the maximum adsorption capacity of the synthesized adsorbent nanomaterials.[6–9]

Information about the ideal adsorbate/adsorbent interaction are obtain by the following non-linear Langmuir equation:

$$q_e = \frac{Q_o b C_e}{1 + bC_e} \quad (5)$$

where q_e (mg g^{-1}) is the content of metal ions adsorbed per unit weight of adsorbate, C_e (mg L^{-1}) is the metal concentration at the equilibrium, Q_0 (mg g^{-1}) is the monolayer capacity and b (mg^{-1} L) represents the constant associated to adsorption heat (K_L). From the K_L parameter it is also possible to calculate the separation factor (R_L) by the equation (6), useful to describe the efficiency of the adsorption process.

$$R_L = \frac{1}{1 + K_L C_0} \quad (6)$$

where K_L is the Langmuir constant and C_0 corresponds to the adsorbate initial concentration (mg L^{-1}). When the R_L=1 a linear adsorption occurs. R_L greater than 1 is associated with unfavourable adsorption, $0 < R_L < 1$ to favourable adsorption, and R_L=0 is referred to irreversible adsorption.

The empirical Freundlich sorption model is usually used to describe non ideal sorption on heterogeneous surfaces as well as multilayer sorption and thus can be applied to fit the adsorption of As(V), Cr(VI) and B(III) onto Fe_3O_4-pVbNMDG following the linear equation (7) here reported:

$$q_e = K_F (C_e)^{\frac{1}{nF}} \quad (7)$$

where K_F (mg g^{-1}) is the Freundlich constant associated with the adsorption capacity and 1/nF is a parameter that allows obtaining indications about the heterogeneity of the system, and thus the intensity of the adsorption.

Temkin equation is a logarithmic isotherm model that takes into account the adsorbate/adsorption interaction on solid surface. It assumes that the heat of adsorption (ΔH_{ads}) of all interacting molecules linearly decreases by increasing the surface coverage. The linear form of Temkin equation is given by:

$$q_e = B_T \ln (K_T C_e) \quad (8)$$

where K_T represents the equilibrium binding constant (L mol^{-1}) that corresponds to the maximum binding energy.B_T is a parameter associated to the heat of adsorption and is defined by

$$B_T = \frac{RT}{b_T} \quad (9)$$

with R the ideal gas constant (8.314 J mol^{-1} K^{-1}), T the temperature in Kelvin and b_T is the parameters related to the variation of adsorption energy (kJ mol^{-1}).

A more general equation than the Langmuir model is the Dubinin-Radushkevich semiempirical equation used to describe sorption curve related to the porous structure of the sorbent. This isotherm model is usually applied to distinguish the physical and chemical adsorption of adsorbate ions onto heterogenous surface. The linear form of the equation is expressed as follows:

$$q_e = q_m exp\left\{ -\beta R^2 T^2 \left[\ln\left(1 - \frac{1}{C_e}\right)\right]^2 \right\} \quad (10)$$

where β is the Dubinin-Radushkevich constant, R the ideal gas constant (8.314 J mol^{-1} K^{-1}), T is the absolute temperature. From equation (10) it is possible to calculate the Polanyi potential (ε) and the adsorption energy (E_{D-R}) that are given by:

$$\varepsilon = RTln\left(1 - \frac{1}{C_o}\right) \quad (11)$$

$$E_{D-R} = 2\beta^{-1/2} \quad (12)$$

The E_{D-R} value can be used to determine the type of adsorption observed. If is below 8 kJ mol^{-1}, typically physical adsorption occurs. Instead, a value between 8 and 16 kJ mol^{-1} indicate the ion-exchange process. Finally, value of E_{D-R} higher than 16 kJ mol^{-1} represented a chemisorption process.[9,10]

As(V), Cr(VI) and B(III) adsorption kinetic profiles

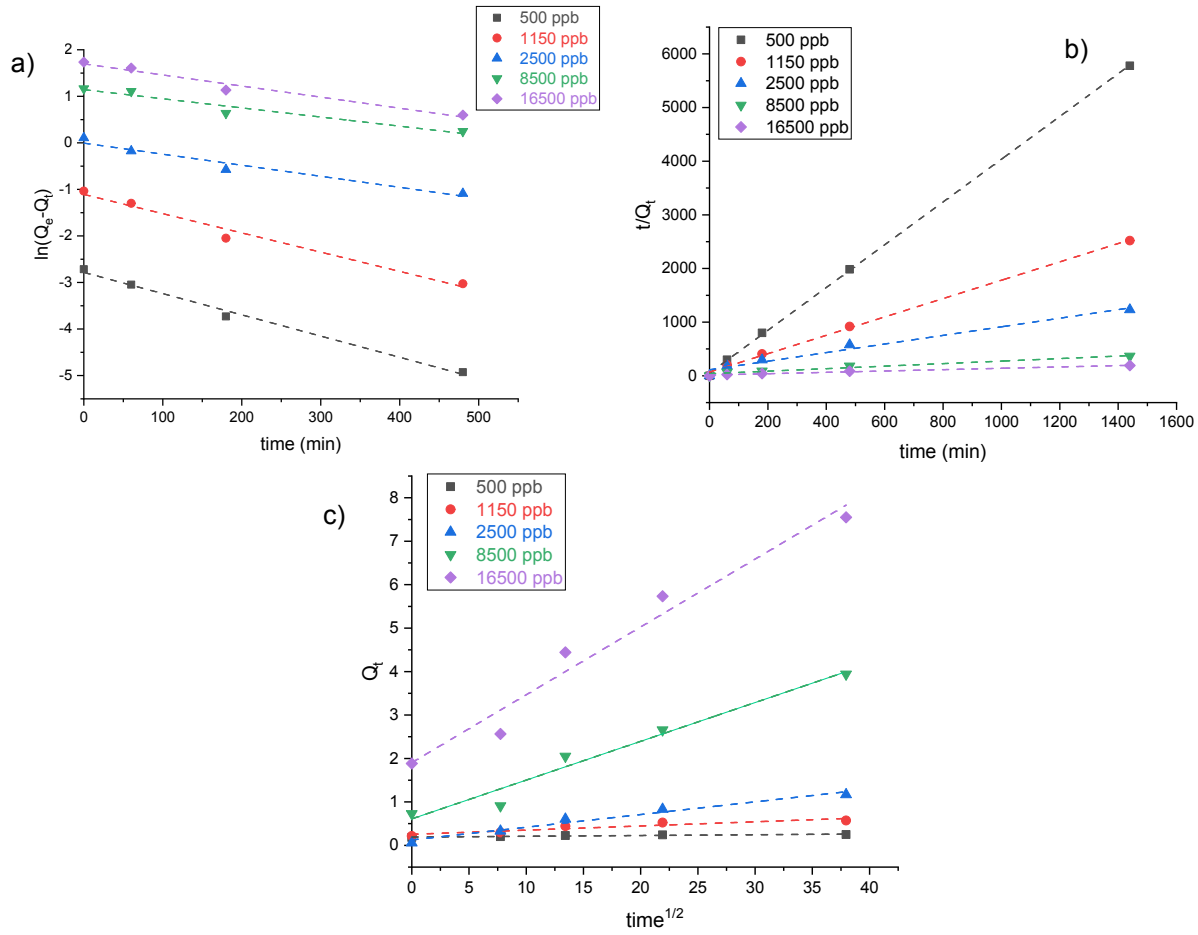

*Figure S11:Adsorption kinetic models of As(V) for poly-VbMEG loaded on Fe_3O_4 fitted with **(a)** the pseudo-first order, **(b)** the pseudo-second order and **(c)** the intraparticle diffusion models*

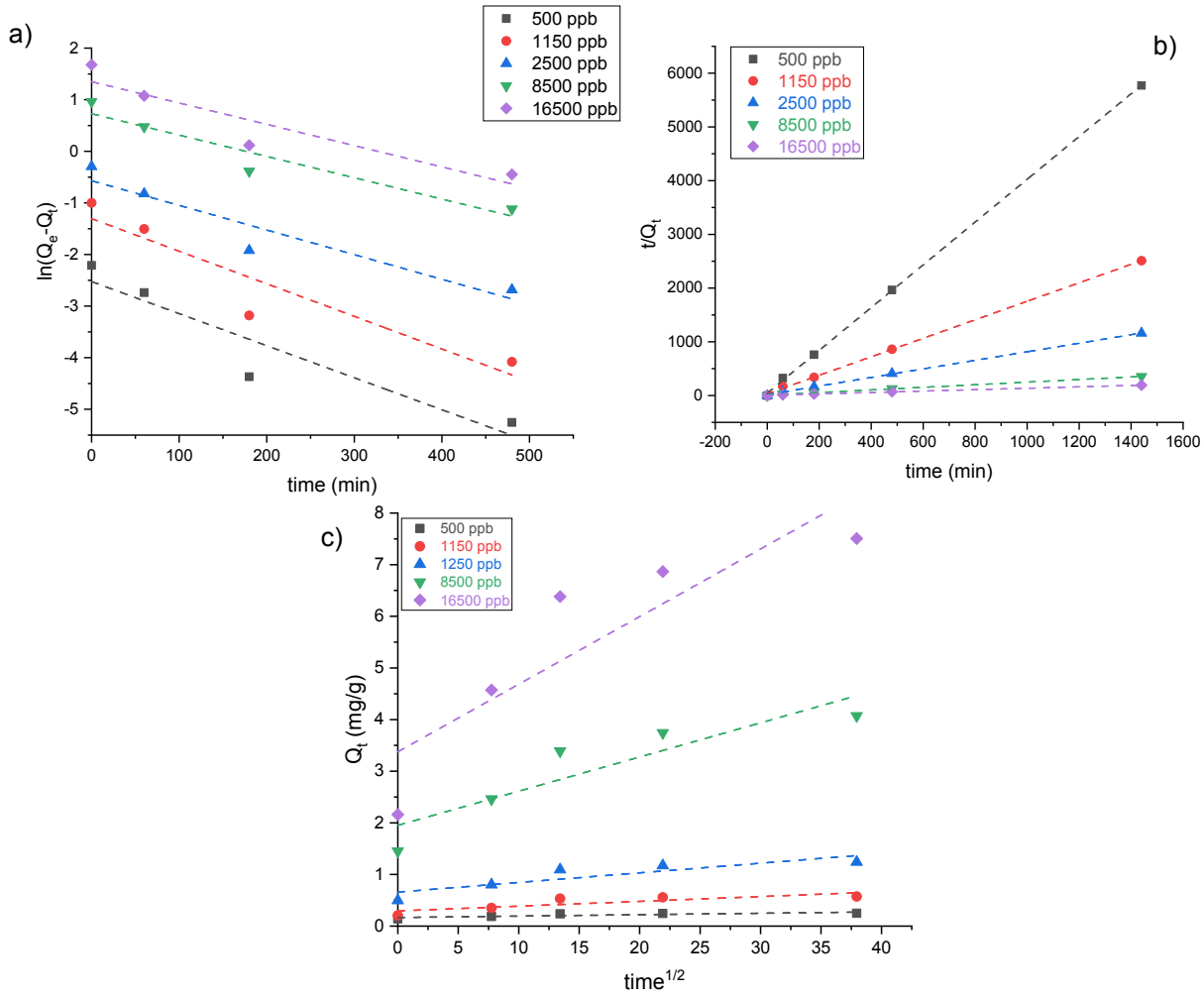

*Figure S12:Adsorption kinetic models of Cr(IV) for poly-VbMEG loaded on Fe_3O_4 fitted with **(a)** the pseudo-first order, **(b)** the pseudo-second order and **(c)** the intraparticle diffusion models*

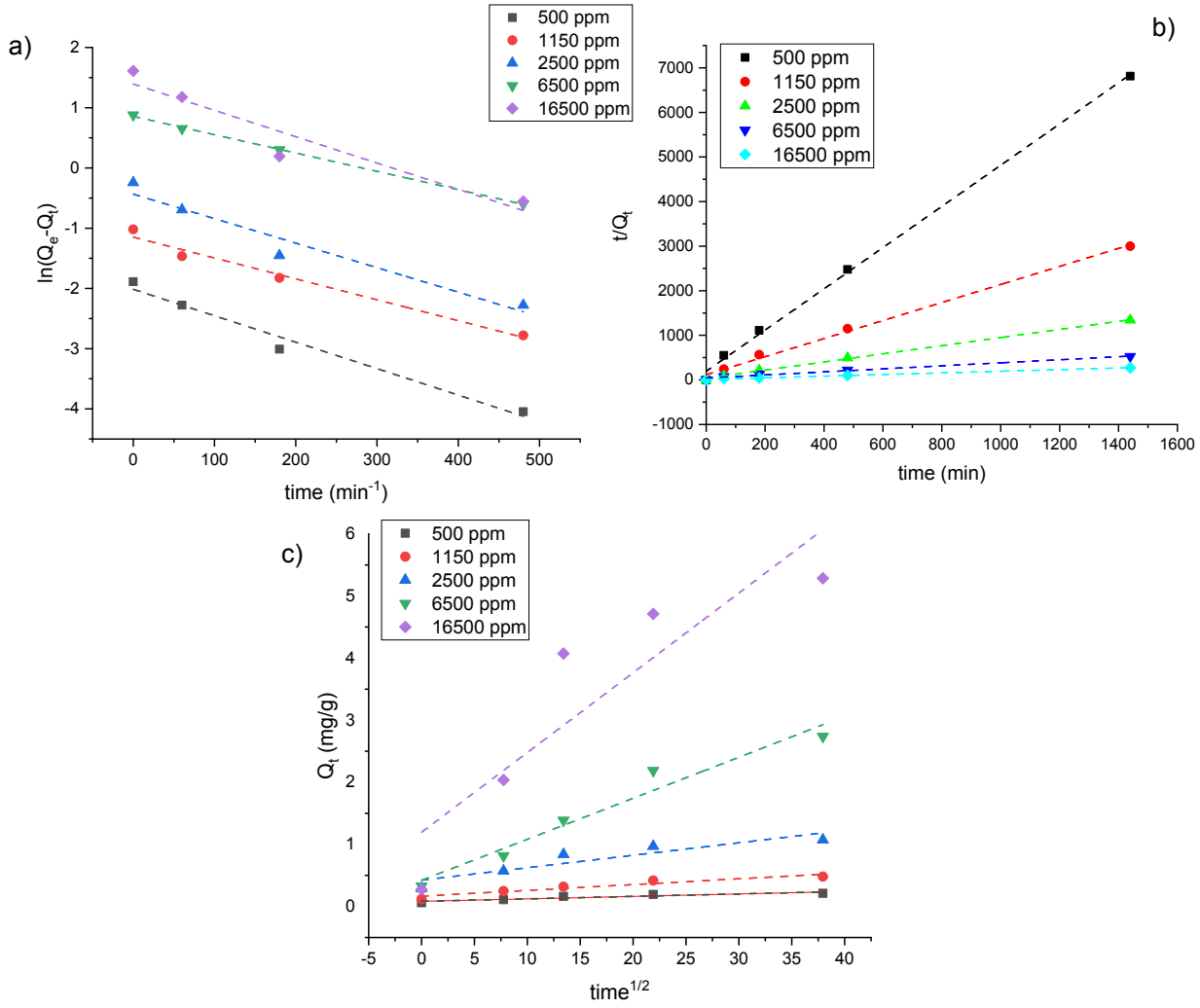

Figure S13:Adsorption kinetic models of B(III) for poly-VbMEG loaded on Fe_3O_4 fitted with ***(a)*** *the pseudo-first order,* ***(b)*** *the pseudo-second order and* ***(c)*** *the intraparticle diffusion models*

References

(1) Mecca, T.; Ussia, M.; Caretti, D.; Cunsolo, F.; Dattilo, S.; Scurti, S.; Privitera, V.; Carroccio, S. C. N-Methyl-D-Glucamine Based Cryogels as Reusable Sponges to Enhance Heavy Metals Removal from Water. *Chem. Eng. J.* **2020**, *399*, 125753. https://doi.org/10.1016/j.cej.2020.125753.

(2) Vrandečić, N. S.; Erceg, M.; Jakić, M.; Klarić, I. Kinetic Analysis of Thermal Degradation of Poly(Ethylene Glycol) and Poly(Ethylene Oxide)s of Different Molecular Weight. *Thermochim. Acta* **2010**, *498* (1–2), 71–80. https://doi.org/10.1016/j.tca.2009.10.005.

(3) *Adsorption Processes for Water Treatment and Purification*; Bonilla-Petriciolet, A., Mendoza-Castillo, D. I., Reynel-Ávila, H. E., Eds.; Springer International Publishing: Cham, 2017. https://doi.org/10.1007/978-3-319-58136-1.

(4) Ho, Y. Review of Second-Order Models for Adsorption Systems. *J. Hazard. Mater.* **2006**, *136* (3), 681–689. https://doi.org/10.1016/j.jhazmat.2005.12.043.

(5) Sutherland, C.; Venkobachar, C. A Diffusion-Chemisorption Kinetic Model for Simulating Biosorption Using Forest Macro-Fungus, Fomes Fasciatus. 12.

(6) Alberti, G.; Amendola, V.; Pesavento, M.; Biesuz, R. Beyond the Synthesis of Novel Solid Phases: Review on Modelling of Sorption Phenomena. *Coord. Chem. Rev.* **2012**, *256* (1–2), 28–45. https://doi.org/10.1016/j.ccr.2011.08.022.

(7) Ramos Guivar, J. A.; Bustamante D., A.; Gonzalez, J. C.; Sanches, E. A.; Morales, M. A.; Raez, J. M.; López-Muñoz, M.-J.; Arencibia, A. Adsorption of Arsenite and Arsenate on Binary and Ternary Magnetic Nanocomposites with High Iron Oxide Content. *Appl. Surf. Sci.* **2018**, *454*, 87–100. https://doi.org/10.1016/j.apsusc.2018.04.248.

(8) Kabay, N.; Sarp, S.; Yuksel, M.; Arar, Ö.; Bryjak, M. Removal of Boron from Seawater by Selective Ion Exchange Resins. *React. Funct. Polym.* **2007**, *67* (12), 1643–1650. https://doi.org/10.1016/j.reactfunctpolym.2007.07.033.

(9) Bessaies, H.; Iftekhar, S.; Doshi, B.; Kheriji, J.; Ncibi, M. C.; Srivastava, V.; Sillanpää, M.; Hamrouni, B. Synthesis of Novel Adsorbent by Intercalation of Biopolymer in LDH for the Removal of Arsenic from Synthetic and Natural Water. *J. Environ. Sci.* **2020**, *91*, 246–261. https://doi.org/10.1016/j.jes.2020.01.028.

(10) Ayawei, N.; Ebelegi, A. N.; Wankasi, D. Modelling and Interpretation of Adsorption Isotherms. *J. Chem.* **2017**, *2017*, 1–11. https://doi.org/10.1155/2017/3039817.